Automatic detection of scleroderma patterns in nailfold capillaroscopy images

Niraj Doshi[1]
n.doshi@lboro.ac.uk
Bartosz Krawczyk[2]
bartosz.krawczyk@pwr.wroc.pl
Gerald Schaefer[1]
gerald.schaefer@ieee.org
Arcangelo Merla[3]
amerla@unich.it

[1] Department of Computer Science, Loughborough University, U.K.
[2] Department of Systems & Computer Networks, Wroclaw University of Technology, Poland.
[3] Institute of Advanced Biomedical Technologies, University of Chieti-Pescara, Italy.

Abstract

Morphological alternations of blood capillaries in the finger nailfold are indicative of underlying connective tissue diseases. This requires close observation of the capillaries, which can be conducted using nailfold capillaroscopy (NC) which is a standard method for diagnosing diseases such as scleroderma or Raynaud's phenomenon. Typically, detection of NC scleroderma patterns (early, active, and late) is performed through manual inspection by an expert. In this paper, we present an automated method of analysing nailfold capillaroscopy images and categorising them into NC patterns. A carefully chosen set of texture features is extracted from the images which we then employ in a pattern classification stage. For the latter, we apply an ensemble classifier to arrive at decisions for each captured finger, which in a final stage are aggregated to form a diagnosis for the patient. Experimental results on a set of 56 NC images from 16 subjects demonstrate the accuracy and usefulness of our presented approach.

1 Introduction

Nailfold capillaroscopy (NC) is a non-invasive and affordable medical imaging technique employed to assess the condition of capillaries in the nailfold. It is a reliable method to assess micro blood vessel characteristics and is acknowledged as a standard method for diagnosing diseases such as systemic sclerosis (SSc) [10], Raynaud's phenomenon [3], and other connective tissue diseases such as dermatomyositis, antiphospholipid syndrome [5], and Sjögren's syndrome [20] which lead to morphological alterations of capillaries.

Such morphological changes include enlarged and giant capillaries, haemorrhages, loss of capillaries, disorganisation of the vascular array, and bushy capillaries [4]. Patterns observable in NC images of SSc patients have been described in [14], and have been refined into early, active and late patterns in [2].

These three NC patterns can be characterised as follows (see also Figure 1 for examples):

- **Early (E):** few giant capillaries, few capillary haemorrhages, relatively well preserved capillary distribution, no evidence of loss of capillaries.

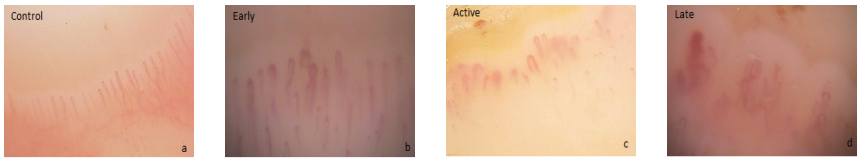

Figure 1: Examples of scleroderma patterns: (a) healthy subject; (b) early; (c) active; (d) late SD pattern.

- **Active (A):** frequent giant capillaries, frequent capillary haemorrhages, moderate loss of capillaries with some avascular areas, mild disorganisation of the capillary architecture, absent or some ramified capillaries.
- **Late (L):** irregular enlargement of the capillaries, few or absent giant capillaries, absence of haemorrhages, severe loss of capillaries with large avascular areas, severe disorganisation of the normal capillary array, frequent ramified/bushy capillaries.

Scleroderma NC patterns are also used to evaluate other rheumatic diseases.

In this paper, we present an automated approach for determining scleroderma patterns from NC images. For this purpose, we extract a set of texture descriptors from the images and employ an ensemble classifier, generated by building multiple support vector machines and combining their results using a neural network fuser. Decisions for individual fingers are then aggregated to form a final diagnosis. Experimental results on a set of 56 NC images from 16 subjects demonstrate the accuracy and usefulness of our presented approach.

2 NC Image Analysis

2.1 Pre-processing

Automated analysis of NC images is challenging due to various factors including image noise, dust on lenses, micro-motion of fingers, and air bubbles in the immersion oil. A first step is therefore to remove noise and enhance the images. Following [7, 8], we apply a bilateral enhancer [9] on the captured images for this purpose.

2.2 Texture analysis

In the few works that attempt to perform automated analysis of NC images [13, 16, 22, 23], single capillaries are extracted and their layout and shape characteristics used for pattern classification. In this paper, we follow a different approach. Not only is exact extraction of capillaries difficult due to the relatively poor image quality (even after enhancement), looking at the examples of Figure 1 again, we can notice that it is possible to distinguish between the different patterns almost 'at a glance'. We therefore employ global image features for analysing and classifying NC images [19].

In particular, we extract texture information from the images and use it in a subsequent classification stage to determine the associated scleroderma patterns. While a variety of texture features exist, those based on local binary patterns [15] have been found to provide excellent performance for a variety of tasks, including texture classification [6]. LBP describes the local neighbourhood of a pixel and, in its basic form, produces 256 texture patterns based on a 3×3 neighbourhood. Neighbouring pixels are set to 0 and 1 by thresholding them with the centre pixel value. The resulting sequence of 0s and 1s is then known as the local binary pattern and a histogram of these patterns over the whole image is generated.

LBP patterns are usually obtained from a circular neighbourhood, while rotation invariance can be obtained by mapping all possible rotated patterns to the same descriptor. Furthermore, certain patterns are fundamental properties of texture and may thus account for the majority of LBP patterns. To address this, only uniform patterns can be utilised where a uniformity measure is defined by the number of transitions from 0 to 1 or vice versa.

Uniform rotation invariant LBP descriptors are powerful texture features [6], however in some preliminary tests we noticed that they did not work as well as we expected for NC images. We consequently employ multi-dimensional LBP (MD-LBP) descriptors as proposed in [18]. MD-LBP calculates LBP features at different scales but preserves their relations by building a multi-dimensional texture histogram.

3 Pattern classification

Uniform rotation invariant MD-LBP texture features, obtained from 3 concentric circular neighbourhoods are extracted from the NC images, and form the basis of a pattern classification stage, where, based on training from known samples, we derive a classifier to identify the scleroderma pattern of an image from its texture characteristics.

Recently, much attention in pattern recognition has been devoted to the development of ensemble classifiers, also called classifier committees or multiple classifier systems [12], and it is such an approach the we employ in this paper. Ensemble classifiers are based on the idea that an appropriately constructed combination of predictors can give better results than any single classifier.

Our proposed ensemble is carefully crafted and consists of three main phases:

1. Creation of a pool of diverse individual classifiers;
2. Pruning the pool by removing redundant predictors;
3. Using a trained fuser based on discriminants to combine the outputs of the classifiers.

In the following, we describe these steps in detail.

3.1 Classifier pool

Individual classifiers used as base models for the committee play a crucial role in the ensemble design process. Instead of using a single feature selection method we employ several of them. We thus generate a diverse pool of classifiers through application of different feature selection algorithms; for L feature selection methods we construct a pool of L individual classifiers $\Pi^{\Psi} = \{\Psi^{(1)}, \Psi^{(2)}, ..., \Psi^{(L)}\}$.

As base classifier, we utilise support vector machines (SVMs) [21] with polynomial kernels, trained using the SMO procedure [17], and employing a tuning procedure to obtain optimal cost and kernel parameters. We use eight different feature selection algorithms, namely ReliefF [26], Fast Correlation Based Filter [25], Tabu Search Wrapper [11], Simulated Annealing Wrapper [11], Forward Selection [11], Backward Selection [11], Quick Branch & Bound [11] and Las Vegas Incremental [11] to generate eight base classifiers.

3.2 Ensemble pruning

In the next stage, we want to ensure that only "valuable" committee members are used for decision making, which we perform based on a diversity measure of the ensemble [1]. In particular, we use a pairwise double-fault diversity measure for this purpose. Given two base

classifiers h_j and h_k, let $n(a,b)$ denote the number of training samples for which the output of these classifiers is a and b respectively; a and b can take on the values 1 (indicating correct classification) and -1 (indicating misclassification) respectively. The double-fault diversity measure can then be calculated as

$$DIV_{DF}(h_j,h_k) = \frac{n(-1,-1)}{n(1,1)+n(-1,1)+n(1,-1)+n(-1,1)}. \tag{1}$$

Diversity for an ensemble of L base classifiers is calculated by averaging the measure over all classifier pairs in the ensemble

$$DIV_{DF}(\Psi) = \frac{2}{L(L-1)} \sum_{j=1}^{L-1} \sum_{k=j+1}^{L} DIV_{DF}(h_j,h_k), \tag{2}$$

which gives measure is in the interval $[0;1]$, where 1 corresponds to a set of identical classifiers and 0 to the highest possible diversity respectively. Classifier selection is achieved by an exhaustive search over all possible combinations of committee members to identify the (pruned) ensemble that minimises the diversity measure function.

3.3 Classifier fusion

For combining the different base classifiers, we employ a trained fuser based on discriminant analysis (as opposed to using the predicted class labels). Assume that we have an ensemble of K classifiers, $\{\Psi^{(1)},\Psi^{(2)},...,\Psi^{(K)}\}$, after the pruning procedure. For a given object $x \in \mathscr{X}$, each individual classifier decides for class $i \in \mathscr{M} = \{1, ...,M\}$ based on the values of discriminants. Let $F^{(l)}(i,x)$ denote a function that is assigned to class i for a given value of x, and that is used by the l-th classifier $\Psi^{(l)}$. The combined classifier Ψ uses the decision rule

$$\Psi(x) = i \quad \text{if} \quad \hat{F}(i,x) = \max_{k \in M} \hat{F}(k,x), \tag{3}$$

where

$$\hat{F}(i,x) = \sum_{l=1}^{K} w^{(l)} F^{(l)}(i,x) \quad \text{and} \quad \sum_{i=1}^{K} w^{(l)}(i) = 1. \tag{4}$$

The weights are set dependent on classifier and class: weight $w^{(l)}(i)$ is assigned to the l-th classifier and the i-th class.

The trained fuser we employ is a neural fuser implemented as a one-layer perceptron [24]. The values of support functions given by each of the base classifiers serve as input, while the output is the weighted support for each of the classes. One perceptron fuser is constructed for each of the classes, and may be trained with any standard procedure used in neural network learning (we use the Quickprop algorithm). The input weights established during the learning process are then the weights assigned to each of the base classifiers.

3.4 Patient classification

For NC diagnosis, typically several fingers are inspected as specific NC patterns might not show on every finger. A decision is thus made based on all fingers and is conducted by a simple majority voting. That is, the class with most decisions is taken as the final results, while in cases of ties we reject a decision.

Table 1: Classification results. Incorrect results are bolded.

Patient	Finger 1	Finger 2	Finger 3	Finger 4	Diagnosis
Control 1	C	C	C	-	C
Control 2	**E**	C	C	C	C
Control 3	**E**	**A**	C	-	**Reject**
Control 4	C	C	C	C	C
Control 5	C	C	C	**E**	C
Early 1	E	E	E	-	E
Early 2	E	E	E	E	E
Early 3	E	E	**C**	-	E
Active 1	**L**	**L**	A	A	**Reject**
Active 2	A	A	A	-	A
Active 3	A	A	A	A	A
Active 4	A	**C**	A	-	A
Late 1	L	L	**A**	-	L
Late 2	**A**	L	L	-	L
Late 3	**E**	L	L	**A**	L
Late 4	L	L	L	L	L

4 Experimental Results

We carried out our experiments on a dataset of 16 subjects with NC images for three to four fingers for each patient. The images were obtained at the Dermatology Unit, Clinical Hospital of Chieti, following their standard protocol. A ground truth for all patients was also obtained by manual inspection carried out by a consultant. Of the 16 subjects, three were found to show early, four active, and four late patterns; the remaining five were control subjects.

Each image is enhanced using a bilateral enhancer and MD-LBP texture descriptors ($MD\text{-}LBP^{riu2}_{1,3,5}$) are extracted. For evaluation, we perform standard leave-one-out cross validation on a patient basis; that is, the classifier is trained on all but one subject for which we run the test, and the procedure is repeated for all patients (i.e., 16 times in total).

The obtained results are summarised in Table 1 where we give both the results of classifying each of the fingers separately and the overall decision for the patient. From Table 1, we can see that in most cases the correct pattern for a finger is identified, namely in 44 of the 56 cases which gives a correct classification of 79% on a per finger basis. When aggregating the individual predictions, the correct patient diagnosis is obtained in all but two cases. In these two cases (Control 3 and Active 1), patient classification is rejected. Overall, it is clear that our approach shows good performance.

5 Conclusions

In this paper, we have presented an approach to analysing nailfold capillaroscopy images with the aim to autmatically identify scleroderma patterns. For this, we extract a set of texture features from the images and employ an ensemble classifier for decision making. Our approach is shown to work well and to give good performance on a test dataset of 56 images from 16 patients. Future work will focus on capturing a larger dataset for evaluation and alternative methods of aggregating individual finger classifications.

References

[1] Y. Bi. The impact of diversity on the accuracy of evidential classifier ensembles. *International Journal of Approximate Reasoning*, 53(4):584–607, 2012.

[2] M. Cutolo, A. Sulli, C. Pizzorni, and S. Accardo. Nailfold videocapillaroscopy assessment of microvascular damage in systemic sclerosis. *The Journal of Rheumatology*, 27(1):155–160, 2000.

[3] M. Cutolo, W. Grassi, and M. Cerinic. Raynaud's phenomenon and the role of capillaroscopy. *Arthritis & Rheumatism*, 48(11):3023–3030, 2003.

[4] M. Cutolo, C. Pizzorni, and A. Sulli. Capillaroscopy. *Best Practice and Research Clinical Rheumatology*, 19 (3):437–452, 2005.

[5] M. Cutolo, A. Sulli, M. E. Secchi, S. Paolino, and C. Pizzorni. Nailfold capillaroscopy is useful for the diagnosis and follow-up of autoimmune rheumatic diseases. a future tool for the analysis of micro-vascular heart involvement? *Rheumatology*, 45 Suppl 4(ii):iv43–iv46, 2006.

[6] N.P. Doshi and G. Schaefer. A comparative analysis of local binary pattern texture classification. In *Visual Communications and Image Processing*, 2012.

[7] N.P. Doshi, G. Schaefer, and A. Merla. Enhancement of nailfold capillaroscopy images. In *IEEE-EMBS Int. Conference on Biomedical and Health Informatics*, 2012.

[8] N.P. Doshi, G. Schaefer, and A. Merla. An evaluation of image enhancement techniques for capillary imaging. In *IEEE Int. Conference on Systems, Man, and Cybernetics*, 2012.

[9] C. Gatta and P. Radeva. Bilateral enhancers. In *16th IEEE International Conference on Image Processing*, pages 3161 –3164, 2009.

[10] W. Grassi, P. D. Medico, F. Izzo, and C. Cervini. Microvascular involvement in systemic sclerosis: Capillaroscopic findings. *Seminars in Arthritis and Rheumatism*, 30(6):397–402, 2001.

[11] I. Guyon, S. Gunn, M. Nikravesh, and L. Zadeh. *Feature extraction, foundations and applications*. Springer, 2006.

[12] L.I. Kuncheva. *Combining pattern classifiers: Methods and algorithms*. Wiley-Interscience, New Jersey, 2004.

[13] H. Kwasnicka, M. Paradowski, and K. Borysewicz. Capillaroscopy image analysis as an automatic image annotation problem. In *6th Interenational Conference on Computer Information Systems and Industrial Management Applications*, 2007.

[14] H. R. Maricq and C. E. LeRoy. Patterns of finger capillary abnormalities in connective tissue disease by "wide-field" microscopy. *Arthritis & Rheumatism*, 16(5):619–628, 1973.

[15] T. Ojala, M. Pietikainen, and T. Maenpaa. Multiresolution gray-scale and rotation invariant texture classification with local binary patterns. *IEEE Transactions on Pattern Analysis and Machine Intelligence*, 24:971–987, 2002.

[16] M. Paradowski, U. Kaczmar, H. Kwasnicka, and K. Borysewicz. Capillary abnormalities detection using vessel thickness and curvature analysis. In *13th Int. Conference on Knowledge-Based and Intelligent Information and Engineering Systems*, pages 151–158, 2009.

[17] J. Platt. Fast training of support vector machines using sequential minimal optimization. In B. Schoelkopf, C. Burges, and A. Smola, editors, *Advances in Kernel Methods – Support Vector Learning*. MIT Press, 1998.

[18] G. Schaefer and N.P. Doshi. Multi-dimensional local binary pattern descriptors for improved texture analysis. In *21st Int. Conference on Pattern Recognition*, pages 2500–2503, 2012.

[19] G. Schaefer, B. Krawczyk, N.P. Doshi, and A. Merla. Scleroderma capillary pattern identification using texture descriptors and ensemble classification. In *35th IEEE EMBS Conference of the IEEE Engineering in Medicine and Biology*, 2013.

[20] M. Tektonidou, E. Kaskani, F. N. Skopouli, and H. M. Moutsopoulos. Microvascular abnormalities in Sjogren's syndrome: nailfold capillaroscopy. *Rheumatology*, 38(9):826–830, 1999.

[21] V. N. Vapnik. *Statistical Learning Theory*. John Wiley & Sons, 1998.

[22] C. Wen, T. Hsieh, W. Liao, J. Lan, D. Chen, K. Li, and Y. Tsai. A novel method for classification of high-resolution nailfold capillary microscopy images. In *1st IEEE International Conference on Ubi-Media Computing*, pages 513–518, 2008.

[23] C. Wen, W. Liao, T. Hsieh, D. Chen, J. Lan, and K. Li. Computer-aided image analysis aids early diagnosis of connective-tissue diseases. In *SPIE Newsroom, Biomedical Optics & Medical Imaging*, 2009.

[24] Michal Wozniak and Marcin Zmyslony. Combining classifiers using trained fuser - analytical and experimental results. *Neural Network World*, 13(7):925–934, 2010. ISSN 1210-0552.

[25] L. Yu and H. Liu. Feature selection for high-dimensional data: A fast correlation-based filter solution. In *20th Int. Conference on Machine Learning*, volume 2, pages 856–863, 2003.

[26] L. Yu and H. Liu. Efficient feature selection via analysis of relevance and redundancy. *Journal of Machine Learning Research*, pages 1205–1224, 2004.